



Obrabotka metallov - Metal Working and Material Science

Journal homepage: http://journals.nstu.ru/obrabotka_metallov







Milling of Inconel 625 blanks fabricated by wire arc additive manufacturing (WAAM)



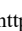

Nikita Martyshev^{1, a, *}, Victor Kozlov^{1, b}, Aleksandr Boltrushevich^{1, c}, Yulia Kuznetsova^{2, d},
Aleksandr Bovkun^{3, e}



¹ National Research Tomsk Polytechnic University, 30 Lenin Avenue, Tomsk, 634050, Russian Federation

² Admiral Ushakov State Maritime University, 93 Lenin Ave., Novorossiysk, 353924, Russian Federation

³ Irkutsk National Research Technical University, 83 Lermontov str., Irkutsk, 664074, Russian Federation

^a  <https://orcid.org/0000-0003-0620-9561>,  martjushev@tpu.ru; ^b  <https://orcid.org/0000-0001-9351-5713>,  kozlov-viktor@bk.ru;

^c  <https://orcid.org/0000-0001-9971-7850>,  aeb20@tpu.ru; ^d  <https://orcid.org/0000-0002-1388-6125>,  julx@bk.ru;

^e  <https://orcid.org/0000-0002-0623-4284>,  Bovas87@yandex.ru

ARTICLE INFO

Article history:

Received: 10 December 2024

Revised: 30 December 2024

Accepted: 23 January 2025

Available online: 15 March 2025

Keywords:

Inconel 625

Wire arc additive manufacturing
(WAAM)

Milling

Cutting forces

Cutting modes

Hardness

Tool wear

Acknowledgements

The research was carried out at the equipment of the Engineering Center “Design and Production of High-Tech Equipment” and the shared research facility “Structure, mechanical and physical properties of materials”.

ABSTRACT

Introduction. Additive manufacturing technologies, in particular wire arc additive manufacturing (WAAM), have been gaining increasing popularity recently. This method allows for the production of blanks with significantly increased hardness compared to traditional methods such as forging, which in turn significantly increases the cutting force during subsequent machining. The present study is aimed at investigating the cutting forces during milling of samples made from the high-strength, heat-resistant alloy *Inconel 625* obtained by WAAM. **The aim of the work** is to investigate the influence of microstructure and properties of *Inconel 625* fabricated by WAAM, on cutting forces during milling. Particular attention is paid to the search for optimal cutting modes, providing minimization of cutting forces and vibrations in the “machine-utility-tool-part” system. **Methods of research.** Samples were produced by WAAM using wire made from heat-resistant nickel-based alloy *Inconel 625*. A comprehensive analysis of the microstructure of the obtained samples was carried out using modern materials science methods. The main attention is paid to the experimental study of cutting forces during milling using different machining modes (cutting speed, feed rate, and depth of cut) and types of cutters. **Results and Discussion.** The microstructure of *Inconel 625* samples obtained by WAAM is characterized in detail. Optimal milling modes will be determined to ensure efficient machining of the material, taking into account its high hardness and strength. It is expected that machining of *Inconel 625* blanks will require high-strength carbide milling cutters, possibly of special geometry and with increased wear resistance, with a larger diameter compared to milling of steel *0.4 C-13 Cr*. The results of the study allow developing recommendations for selecting optimal cutting modes minimizing cutting force, cutting edge temperature, tool wear and vibrations in the “machine-utility-tool-part” system, thereby improving processing productivity and accuracy.

For citation: Martyshev N.V., Kozlov V.N., Boltrushevich A.E., Kuznetsova Yu.S., Bovkun A.S. Milling of Inconel 625 blanks fabricated by wire arc additive manufacturing (WAAM). *Obrabotka metallov (tekhnologiya, oborudovanie, instrumenty) = Metal Working and Material Science*, 2025, vol. 27, no. 1, pp. 61–76. DOI: 10.17212/1994-6309-2025-27.1-61-76. (In Russian).

* Corresponding author

Martyshev Nikita V., Ph.D. (Engineering), Associate Professor
National Research Tomsk Polytechnic University,
30 Lenin Avenue,
634050, Tomsk, Russian Federation
Tel.: +7 3822 60-62-85, e-mail: martjushev@tpu.ru

Introduction

Modern development of science and technology stimulates active implementation of innovative technologies in various fields, including the production of metal parts. Additive technologies, despite their considerable potential, still face the problems of low productivity and high cost. The desire to optimize these processes has led to the development of additive manufacturing methods based on metal wire deposition [1–3].

This approach, compared to the use of powder materials, significantly reduces the fabrication time and lowers the cost of blanks due to the lower price of wire. However, the wire deposition method often results in insufficient surface quality, requiring additional machining. In addition, specific cooling conditions during the wire deposition process result in a microstructure with increased hardness compared to conventional manufacturing methods such as forging or casting. This is especially true when heat-resistant materials are used [4, 5]. To demonstrate the advantages and disadvantages of the cladding method, let us consider a high-strength, heat-resistant alloy — *Inconel 625*. Its high cost and specific properties allow us to demonstrate the advantages and disadvantages of this method. The high hardness achieved when depositing *Inconel 625* wire necessitates specialized machining methods aimed at optimizing processes and minimizing costs [6–8].

In the layer-by-layer wire deposition process, each new layer is deposited on the previous layer, which in turn undergoes repeated heating and rapid cooling [9]. This heating and cooling cycle has a significant effect on the formation of the microstructure. In the case of martensitic steels, a relatively low critical cooling rate favors the formation of a martensitic structure with high hardness, as confirmed by studies [10, 11]. However, when selective laser melting (*SLM*) or wire arc additive manufacturing (*WAAM*) is used with *Inconel*, the situation becomes more complicated. Due to high melting temperatures and complex phase transformations, there is anisotropy of mechanical properties in the finished part. Grain size, porosity, and consequently, strength properties depend on the direction of measurement, as shown in the works [12, 13]. This is attributed to the non-uniform thermal cycle during the layer-by-layer build process. Work [14] demonstrates the anisotropy of the mechanical properties in parts fabricated by additive methods, and work [15] indicates the possibility of partial compensation for this effect through heat treatment, which, however, increases production costs. Furthermore, rapid cooling during *SLM* or *WAAM* can lead to the formation of a hardened surface layer with extremely high hardness on the surface of workpieces made from heat-resistant alloys, which significantly complicates subsequent machining. For *Inconel*, this effect can be even more pronounced due to its unique properties and higher melting temperature.

The parameters of the wire arc additive manufacturing (*WAAM*) process, such as substrate temperature, torch speed, and trajectory [16–17], significantly affect the microstructure formation and, consequently, the mechanical properties of the resulting workpiece. Even when these parameters are optimized, structural defects such as local surface hardening, inhomogeneity of phase distribution, and micropores inevitably occur, which reduces the predictability of mechanical properties. *WAAM*, as one of the additive manufacturing methods, is characterized by the formation of an anisotropic microstructure with non-uniform distribution of stresses and properties over the part volume [18–20]. This is due to the layer-by-layer nature of the wire depositing, non-uniform heating and cooling, and internal stresses arising during melt crystallization.

In addition to the inhomogeneity of the structure, *WAAM* technology often leads to the formation of workpieces with poor surface quality, requiring mandatory subsequent machining [21–23]. Grain size, porosity, and consequently, strength properties depend on the direction of measurement, as shown in [12, 13]. This is due to the inhomogeneity of the thermal cycle during the layer-by-layer build-up process. The work of [14] demonstrates the anisotropy of the mechanical properties of products fabricated by additive methods, while the work of [15] indicates that it is possible to partially compensate for this effect by heat treatment, which, however, increases the manufacturing costs.

The complex thermal cycles inherent in *WAAM* technology result in the formation of an inhomogeneous microstructure in the obtained billets, which significantly complicates subsequent machining. This heterogeneity is manifested in significant variations in hardness, strength, and other mechanical properties

throughout the volume of the part, especially pronounced when using heat-resistant alloys. Work [26] has shown that milling of *WAAM*-produced Ti_6Al_4V alloy workpieces results in significant tool wear (e.g., Al_2O_3/Si_3N_4 sialon end milling cutter) compared to machining forged or cast specimens. This increased abrasiveness is due to both the heterogeneity of the microstructure and the presence of residual stresses arising from the wire depositing process. The increased hardness of locked zones, microcracks, and uneven phase distribution contribute to the rapid cutting tool wear. To reduce wear and increase tool life when machining heat-resistant alloys produced by *WAAM*, several strategies can be employed [27, 28]. These include optimizing cutting parameters (cutting speed, feed rate, depth of cut), utilizing modern high-strength and wear-resistant tool materials, and employing effective cooling systems, such as cryogenic cooling. The selection of an optimal strategy depends on the specific heat-resistant alloy, the required machining quality, and economic considerations. It is crucial to consider that for heat-resistant alloys characterized by high hardness and strength, enhanced tool life is a critical factor affecting productivity and economic efficiency of the machining process [29].

One approach to reduce tool wear when machining parts produced by *WAAM* is to optimize the wire depositing process parameters to obtain the required surface properties. By controlling the process parameters (wire depositing speed, electron beam parameters, substrate temperature, etc.), it is possible to influence the microstructure formation and, consequently, the hardness and abrasiveness of the surface. This is especially relevant for heat-resistant alloys, where the inhomogeneity of the structure determines the intensity of tool wear. To quantitatively analyze the microhardness heterogeneity in heat-resistant alloy billets obtained by *WAAM*, special data aggregation techniques have been developed and applied to estimate the average hardness values and their variations in different zones of the part [30]. This approach makes it possible to predict tool wear more accurately and optimize machining modes.

The use of combined additive manufacturing techniques, combining different wire depositing technologies or adding intermediate processing steps, can help to obtain a more homogeneous structure and thus improve the machinability of heat-resistant alloys. However, despite these efforts, studies [31] show that machining of heat-resistant alloy blanks produced by additive manufacturing methods (*WAAM*, *SLM*, etc.) is often accompanied by an increase in cutting forces compared to machining of parts produced by traditional methods (forging, casting). This is explained not only by the inhomogeneity of the structure, but also by the presence of residual stresses, micropores, and other defects characteristic of additive technologies. The work [31] confirms the high variability of cutting forces when machining *WAAM* blanks, even when using the same machining modes, which emphasizes the importance of individual selection of cutting parameters for each specific part.

There is very limited research on subtractive machining of parts produced by wire arc additive manufacturing (*WAAM*). This is due to a number of factors, including the difficulty in predicting material properties after wire depositing and the need for specific machining methods that take into account microstructure features. In particular, the use of *WAAM* to create workpieces from heat- and corrosion-resistant alloys such as *Inconel 625* presents additional challenges due to the high hardness and strength of the material. Therefore, the development and optimization of machining modes for *Inconel 625* billets produced by the *WAAM* method is an urgent task requiring a comprehensive approach. The need to determine optimal cutting parameters to minimize tool wear, increase productivity, and ensure the required surface quality makes this topic particularly significant for the development of additive technologies and their industrial applications.

The **aim of this work** is to determine the milling modes for *Inconel 625* workpieces produced by wire arc additive manufacturing (*WAAM*) through conducted research.

Materials and methods

Five specimens were printed to investigate the cutting forces generated during the machining of *Inconel 625* workpieces produced by wire arc additive manufacturing (*WAAM*). The geometric dimensions of each specimen were 25 mm (height) \times 75 mm (width) \times 25 mm (length). This shape and dimensions

were selected to ensure sufficient rigidity of the samples during milling and to minimize the influence of fixturing on the experimental results. The use of standardized dimensions allows the results to be compared with data from other studies.

The specimens were fabricated by *WAAM* using *Inconel 625* wire (the alloy composition is provided in Table). The choice of *Inconel 625* is due to its wide application in high-temperature conditions and its complex microstructure, which allows us to investigate the influence of the *WAAM* process on the mechanical properties and machinability of the material. To ensure the reproducibility of the results, the wire depositing process was carried out using strictly controlled parameters (wire depositing speed, arc voltage, shielding gas flow rate, etc.) optimized to produce the minimum number of defects and the most homogeneous microstructure possible. These parameters will be described in detail in the relevant section of the study.

Chemical composition of Inconel 625 nickel alloy wire

Chemical element	Ta	Al	Nb	Mo	Cr	Si	Fe	Co	Ti	Mn	Ni
%	0.3	0.38	2.8	7.5	22.5	0.8	1.3	0.2	0.35	0.1	63.68

Fabrication of samples by wire arc additive manufacturing (WAAM)

The samples were printed using a wire arc additive manufacturing machine. This equipment was developed and manufactured at Tomsk Polytechnic University. Manufacturing of *Inconel* specimens by the wire arc additive manufacturing (*WAAM*) method was carried out according to the following technology. First, a 3D computer model was created using a *CAD* system. Then this model was divided into separate layers, each of which was to be deposited.

The layer-by-layer wire depositing process was carried out on a 3D printer using the specified parameters: current was 115–135 A, voltage 21–24 V, and wire depositing speed was 300 mm/min. An inverter rectifier was used as a power source, which provides high process stability and control of surfacing parameters. Wire depositing was carried out on a moving table, providing precise positioning in *X* and *Y* axes, which guarantees accurate reproduction of the geometrical parameters of the model. The *Z*-axis positioning of the depositing torch was controlled for accurate and homogeneous layers' depositing. The melting of the wire and the fusion of the substrate (or previous layer) took place using a controlled trajectory of the torch, guaranteeing accurate wire depositing and minimal deviation from the model. The thickness of the wire depositing layer varied from 2 to 5 mm depending on the selected wire depositing modes and the required accuracy. The specified wire depositing modes were optimized to achieve the desired quality and minimum defects, suitable for subsequent stages of the study. For the printing process, the substrate material was the same as the wire: a heat-resistant nickel-based alloy. Printing was carried out in an argon shielding gas environment.

Investigation of microstructure and hardness of the obtained samples

Chemical etching was carried out to reveal microstructural features of *Inconel 625* samples fabricated by wire arc additive manufacturing. The etching process was carried out by immersing the samples in a specially prepared etching solution for 8 minutes. The solution was a mixture of hydrochloric acid (10 ml), hydrofluoric acid (10 ml), and ethanol (100 ml). This particular etchant composition was chosen due to its effectiveness in revealing microstructural details of nickel alloys such as *Inconel 625*, providing sufficient contrast between the different phases and grain boundaries. After etching, the samples were thoroughly rinsed with distilled water and dried with compressed air to prevent corrosion and ensure high precision of analysis. The samples obtained after etching were examined using a *Carl Zeiss AxioMAT* optical microscope, which provides high resolution and measurement accuracy. The use of this microscope allowed obtaining detailed images of the microstructure, including analysis of grain size and shape, identification of dendritic structure, determination of the presence of secondary phases and other structural inhomogeneities, which are

directly related to the parameters of the wire arc additive manufacturing process and affect the mechanical properties of the material. The resulting micrographs were used to quantitatively analyze the microstructure, including measuring grain size, determining the degree of dendritic structure, and estimating the volume fraction of secondary phases.

Study of cutting forces in milling operations

The experimental study of milling was carried out on a high-precision CNC-controlled machining model *CONCEPTMill 155*, manufactured by *EMCO*. This model was chosen because of its high rigidity, positioning accuracy, and the possibility of conducting controlled experiments. A highly sensitive six-component dynamometer *Kistler 9257B* (Switzerland) was used for precise measurement of cutting forces during milling. This sensor has high sensitivity (7.5 N) and low measurement error ($\pm 0.005\%$), which ensured the reliability of the obtained data. Processing and analysis of experimental data were carried out with the help of specialized software *DynoWare*, which allows carrying out complex analysis of cutting forces, to reveal their dynamic characteristics, and to take into account the influence of various machining parameters. The total variation in cutting force measurements was limited to 15 %, primarily attributed to challenges in precisely controlling milling parameters (cutting width and depth) and to the unavoidable tool wear resulting from repeated experiments.

A carbide end mill with a diameter of 8 mm produced by *MION* was chosen as the cutting tool. This end mill was chosen for its high strength and wear resistance, essential for machining the high-strength and abrasive *Inconel 625* alloy. The carbide material of the cutter consisted primarily of tungsten carbides, which provide high hardness and wear resistance of the cutting edge, and a cobalt binder (approximately 8 %), which is responsible for the strength and cohesion of the carbide grains. The end mill design included four teeth, which provided a sufficient material removal rate but required careful control of cutting parameters to prevent overheating and vibrations. The geometry of the end mill (sharpening angle, front and back angles) was standard for this type of tool and was not modified for this study. This particular tool was chosen due to its availability, well-studied characteristics, and suitable parameters for this study. The helix angle (ω) was 35° , the back angle was 5° , and the front angle was 7° . Dry milling was employed in the experiments.

Results and Discussion

Fabrication of Samples by wire arc additive manufacturing (WAAM) and Subsequent Microstructural Characterization

Samples were initially fabricated for this investigation. Five samples were obtained using *WAAM* technology to carry out the required amount of research. The photograph of the obtained billet and the scheme of sampling for metallographic studies are shown in Fig. 1.

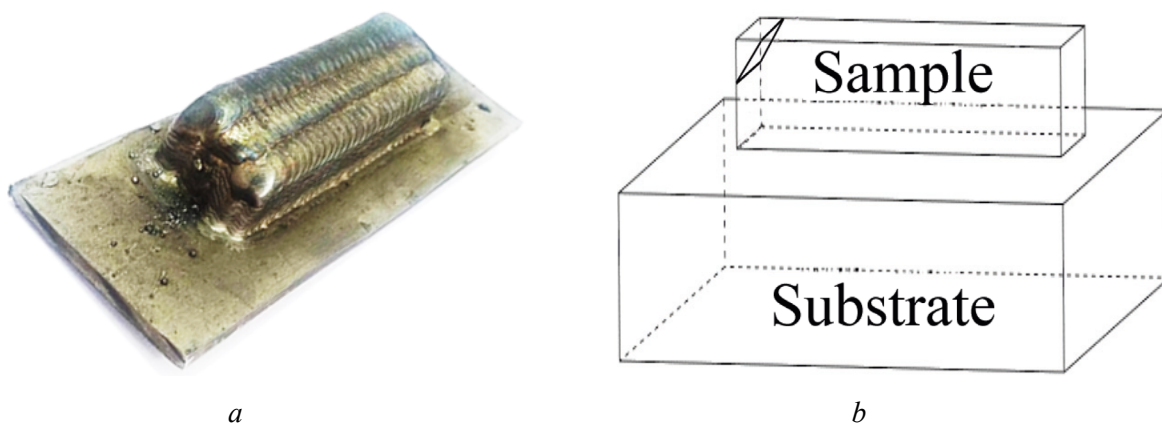


Fig. 1. Photograph of a printed workpiece (a) using *WAAM* technology and a diagram of the sample cutout (b) for research



Fig. 2. Microstructure of the samples obtained using WAAM technology

The microstructure of the samples from *Inconel 625* obtained by wire arc additive manufacturing (WAAM) technology is shown in Fig. 2. The micrograph obtained with an optical microscope clearly shows an elongated, cellular structure in the centre of the sample. A characteristic feature is the presence of bright inclusions (probably secondary phases or oxide particles) in the intergranular regions (between dendrites). This indicates the complexity of phase transformations and possible inhomogeneities occurring during the wire depositing process. The dendritic structure is also clearly visible in the image. Dendrites formed during solidification of molten *Inconel* have prominent first-order axes extending in one direction. The second-order axes are usually much less pronounced or absent, indicating the specificity of crystallisation caused by rapid wire

depositing processes. This microstructure feature is related to the high cooling rates characteristic of WAAM. In addition, the microstructure analysis indicates a noticeable texture in the grains. The presence of texture may indicate the preferred directions of crystallite growth due to the directional heat flow and stress state of the material during wire depositing. These texture and dendritic structure features significantly affect the mechanical properties of the finished WAAM-derived *Inconel 625* samples.

The different cooling rates characteristic of the wire arc additive manufacturing (WAAM) process result in the formation of different grain sizes in the *Inconel 625* samples. The microstructure is characterised by a dendritic structure where the crystals are elongated along the direction of heat dissipation. This direction coincides with the direction of layer build-up during WAAM. A pattern of grain size increase with distance from the substrate is observed. In the studied samples, the length of dendrites reached 0.3–0.5 mm. This is consistent with the data of other researchers studying the microstructure of *Inconel 625* obtained by additive methods. For example, in the study [6] a grain size of approximately 1 mm was observed in *Inconel 625* samples produced using selective laser melting (SLM). The difference in grain size can be explained by the different cooling rates characteristic of WAAM and SLM. The results also confirm the data of [11, 16], where it is shown that in the lower part of the *Inconel 625* sample (closer to the substrate), equiaxed grains predominate. As the distance from the substrate increases and new layers are deposited, the grains elongate along the direction of heat extraction, texture develops, and their length significantly increases. The coincidence of the observed patterns with the results of [11, 16] confirms the results and allows us to conclude about the influence of heat flow and cooling rate on the formation of microstructure in *Inconel 625* samples obtained by WAAM method.

Microhardness

The microhardness of the samples was determined using the *Vickers* method at a 1 kgf load with a dwell time of 10 s. Values were calculated as the average of twenty indentations at different locations.

Microhardness measurements (Fig. 3) indicate that the hardness at the center of the samples is lower compared to the edges. The central areas of the sample cool more slowly than the peripheral ones. The outer areas, dissipating heat more rapidly to the surrounding environment, solidify faster, resulting in a finer-grained microstructure and consequently higher hardness. Conversely, the central areas cool more slowly, promoting the growth of larger grains and leading to a reduction in hardness. This aligns favorably with the results of our metallographic analysis. This structural variation will influence the processing parameters of the workpieces and the cutting forces generated during machining.

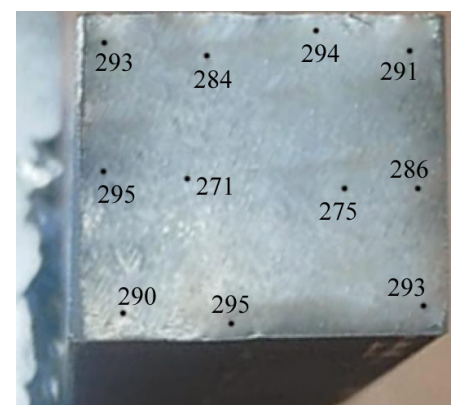


Fig. 3. Microhardness of the samples obtained using WAAM technology

Study of cutting forces during sample machining

The experimental results presented below focus on the analysis of cutting forces during the milling of *Inconel 625* specimens produced by wire arc additive manufacturing (*WAAM*). The aim of the experiment was investigating the influence of cutting modes on cutting forces in *WAAM*-processed material with high hardness and heterogeneous microstructure.

To maintain controlled experimental conditions, the milling width (B) was held constant at 2 mm throughout the experiment series. This ensured that with a small milling depth ($t = 1$ mm), only a single cutting tooth was engaged at any given time, allowing for the acquisition of cutting force profiles on a per-tooth basis as the cutter rotated (Fig. 5).

The presence of the angle of inclination of the helical line of the main cutting edge of the tooth at the periphery of the cutter $\omega = 40^\circ$ (sometimes the symbols β or ψ are used) also forces to reduce the milling width B . When increasing the milling width B , the next tooth may start cutting, although the previous tooth has not yet finished cutting. This factor is more important for small diameter milling cutters ($d_{\text{cutter}} < 12$ mm) and when the milling depth $t > 0.4 \cdot d_{\text{cutter}}$ is increased.

Minute feed (f_{min}) was chosen as the main variable cutting parameter in the series of experiments under consideration, while other cutting parameters (cutting depth t , cutting speed V) were constant. This approach allowed us to evaluate the influence of the minute feed rate on the value of cutting forces in isolation from other factors.

The data on cutting forces obtained during the experiment were processed using the least squares method to approximate the empirical relationships. This made it possible to obtain analytical expressions describing the dependence of cutting forces on the minute feed. To visualise the results of the experiment, graphs were plotted showing the maximum values of cutting forces in each machining cycle (Fig. 4). Utilizing maximum cutting force values mitigates the influence of force fluctuations inherent in the milling process on the observed effect of s_{min} . These fluctuations arise from variations in chip thickness during cutter rotation, radial runout of the cutter teeth, material heterogeneity, and minor vibrations within the *machine-tool-workpiece* system. This approach allows to obtain more generalised and reliable results reflecting the general tendency of change of cutting forces depending on the minute feed, moreover, the destruction of a cutter tooth is influenced by the highest force on any tooth.

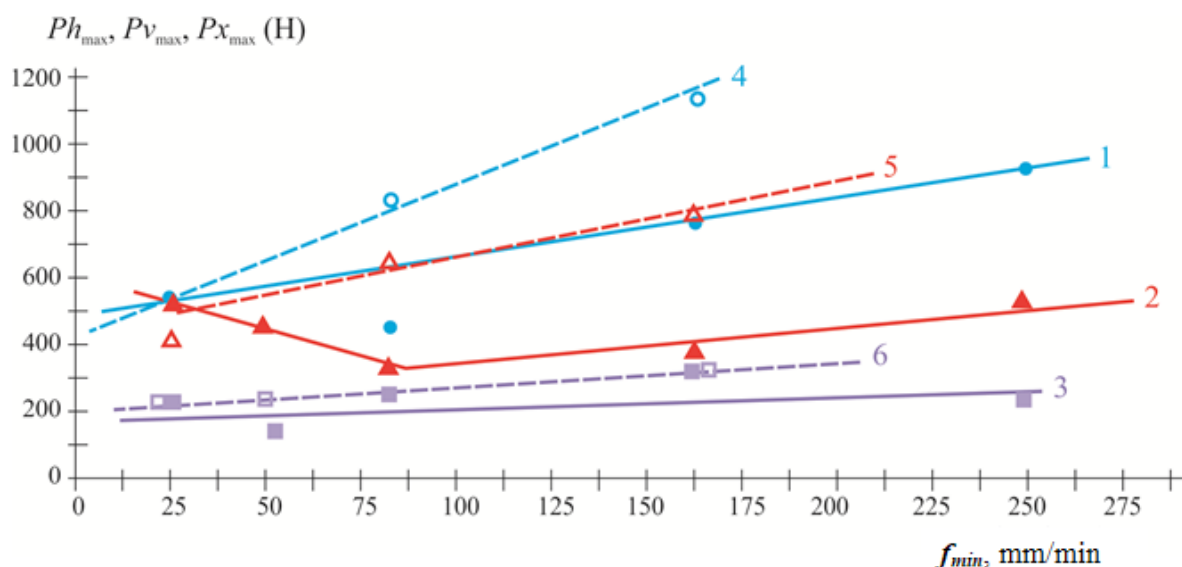


Fig. 4. Graph of the change in the highest values of cutting forces Ph , Pv and Px (N) depending on the feed rate f_{min} (mm/min) ($B = 2$ mm, $V = 15,8$ m/min, $t = 1$ mm)

Feed along the sample: 1 - Ph_{max} , 2 - Pv_{max} , 3 - Px_{max} ; Feed across the sample: 4 - Ph_{max} , 5 - Pv_{max} , 6 - Px_{max}

Fig. 4 illustrates the variation of feed force (P_h), acting along the table feed direction), lateral force (P_v , perpendicular to the feed direction), and axial force (P_x , acting along the milling cutter axis, i.e., vertically in end milling) as a function of minimum chip thickness (f_{min}). When feeding across the specimen, the maximum feed force ($P_{h_{max}}$) and maximum lateral force ($P_{v_{max}}$) are larger, and their increase with increasing feed is more pronounced, indicating an influence of the build direction in *WAAM*. The maximum axial force ($P_{x_{max}}$) remains relatively constant with increasing feed, but exhibits a slightly higher value when feeding across the specimen.

In Fig. 4, graph 2 ($P_{v_{max \text{ along}}}$) exhibits an inflection point at $f_{min} = 80$ mm/min, an effect not observed when feeding across the specimen in graph 5 ($P_{v_{max \text{ across}}}$). Furthermore, at $f_{min} = 80$ mm/min, a decrease in the maximum feed force ($P_{h_{max \text{ along}}}$) is apparent in graph 1; however, the remaining data points for this force lie on a linear trend.

Analysis of the cutting force graphs shown in Fig. 4 reveals characteristic force interactions between the milling cutter and the workpiece. The force vector P_v is measured by a dynamometer with a negative value. This indicates that this force component, which arises from the radial impact of the cutter teeth, is directed away from the operator, i.e., opposite to the OY axis. For ease of visualisation, the vector $P_{v_{max}}$ is shown in the positive direction of the axis in the figure, although its actual direction is opposite. Similarly, the force P_x , also having a negative value, is directed against the OZ axis. This is a consequence of the positive helix angle ω of the milling cutter, which results in a vertical pull-up of the workpiece. It is important to note that the absolute values of the forces P_v and P_x are considered in the analysis, as these reflect the intensity of the force impact. At the same time, the force P_h has a positive value, corresponding to the direction of the OX axis, which defines the primary cutting force.

An analysis of the maximum cutting forces values $P_{h_{max}}$ and $P_{v_{max}}$ as a function of the minimum feed rate f_{min} (see Fig. 4), with a cutting depth of 3 mm and other constant cutting parameters, demonstrates their approximately linear relationship. This allows for the use of linear equations to approximate these dependencies within the considered parameter range. A pattern is observed: when synthesizing workpieces and directing the feed along the machining axis, the values of the maximum forces $P_{h_{max}}$, $P_{v_{max}}$ and $P_{x_{max}}$ are slightly smaller than when the feed direction is perpendicular. This difference, as seen in Fig. 4, is not significant but shows the influence of the feed direction on the force characteristics of the milling process. The difference in force values may be due to changes in the contact conditions between the tool and the workpiece, specifically changes in the contact area of the cutting edge and the depth of cut, depending on the feed direction. Further studies, including analysis of the helix angle of the milling cutter, the geometry of the cutting edge, and the properties of the workpiece material, are needed for a more accurate explanation of this phenomenon. Moreover, some factors, such as the presence of vibrations and the influence of the coolant, may also contribute to the observed differences. A more accurate model, considering all these factors, will allow for more precise prediction of force characteristics and optimization of the technological process.

Fig. 5 demonstrates an unexpected phenomenon during milling with a four-tooth tool at a cutting depth of 3 mm. Despite the theoretical assumption of only one tooth is in contact with the workpiece at any given time, which should lead to periodic zeroing of the cutting force, continuous force exertion is observed, most prominently expressed in the feed force (P_h) graph (purple curve). Moreover, the increase in the minimum P_h value with increasing feed rate indicates a complex interaction between the tool and the workpiece that goes beyond a simple single-tooth cutting model.

Analysis of the P_h cutting force curve reveals a distinct pattern of four pronounced peaks and valleys. This periodicity unequivocally indicates that all four teeth of the milling cutter participate in the cutting process, each leaving its imprint on the curve. Small but noticeable amplitude variations of these peaks are observed, indicating a slight radial runout of the teeth. However, it is important to note that the maximum P_h values for adjacent teeth are almost identical. This equality of amplitudes for adjacent teeth suggests that the radial distance of each tooth from the axis of rotation of the milling cutter is the same. This fact allows us to confidently rule out any displacement of the milling cutter axis relative to the collet chuck as the cause of the recorded cutting force fluctuations.

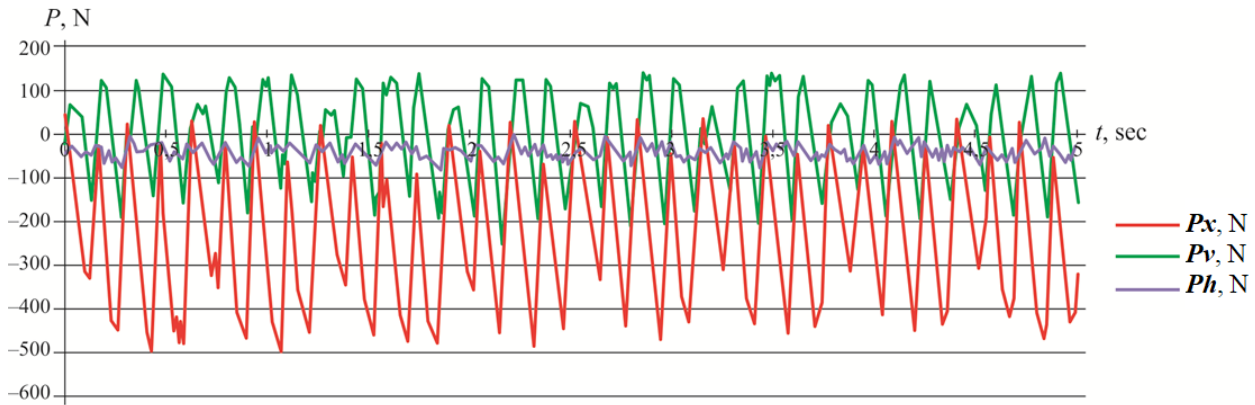


Fig. 5. Example of a graph showing the change in force components over cutting time during milling process along the growing direction ($B = 2$ mm, $V = 16$ m/min, $t = 1$ mm, $f_{min} = 25$ mm/min)

Thus, we conclude that the identified irregularities in the cutting force characteristics are the result of manufacturing deviations made during the production of the milling cutter. These deviations likely involve imperfections in the tooth geometry or inaccuracies in their placement. At the same time, it can be stated that the installation and fixation of the milling cutter in the chuck are performed correctly and are not the cause of the observed phenomenon. A detailed study of the Ph force variation curve, which demonstrates a clear repeatability of peaks and valleys, confirms this conclusion, allowing further analysis to focus on the technological aspects of the tool manufacturing process. A more detailed analysis of the cutter geometry is necessary to determine the exact causes of these deviations from the ideal geometry and to assess their impact on the quality of machining and the dimensional accuracy of the resulting part.

Analysis of the cutting force dynamics of Ph (see Fig. 4), which is the most informative and easily observable component of the force interaction, reveals approximately symmetrical patterns of its increase and decrease during conventional milling. This is somewhat contrary to the expected asymmetry, caused by a significantly shorter period of the tooth exiting the cutting zone compared to the period of its entry. Theoretically, a rapid decrease in the chip thickness before the tooth completely exits should lead to a steeper drop in the Ph force. This is explained by the change in the orientation of the force vector Pz as the tooth approaches the exit point. At the moment preceding the exit of the milling cutter tooth from the contact zone, Pz rotates in the direction of rotation of the milling cutter. This gives a more significant increase in the radial component of the force Py than the force Ph . As a result, the decrease in the Ph force begins earlier — even before the main cutting edge completely leaves the contact zone with the workpiece.

The presence of the cutting edge inclination angle, denoted as ω (or β in some foreign publications), plays a key role in the milling process. This angle prevents the entire cutting edge from simultaneously entering the contact zone with the workpiece or exiting it. Instead of an abrupt cessation of the cutting process, a more gradual process occurs. Individual sections of the cutting edge sequentially exit the interaction with the material. The milling width B and the inclination angle ω have a significant impact on the smoothness of the decrease in all components of the cutting force — axial Px , tangential Pz , and radial Py . The greater the values of these parameters, the smoother and less abrupt the decrease in cutting forces will be when the tooth exits the machining zone. This is explained by the fact that a wider tool and a larger inclination angle provide a more gradual change in the contact area between the tool and the workpiece. A more gradual decrease in cutting forces, in turn, leads to reduced vibrations and improved surface finish.

However, the milling process, especially in conventional milling, involves a complex interaction of several factors. The rotary motion of the milling cutter, the changing orientation of the force vectors Pz and Py , and the simultaneous variation in chip thickness a result in a certain phase shift between the changes in forces. This shift manifests itself in the fact that the change in the radial force Py (lateral force Py in Fig. 4) does not perfectly coincide in time with the change in the tangential force Pz (feed force Ph in Fig. 4). This phase shift, although slight, is a consequence of the dynamic processes occurring in the cutting

zone and affects the overall force interaction pattern. Understanding the relationship between the tool's geometrical parameters (ω and B), the process kinematics (cutter rotation), and the cutting force dynamics (P_z , P_y , P_h , P_v) is necessary for optimizing the milling process and achieving the best possible surface finish (see Fig. 5). More accurate process modeling requires considering all these factors, as well as the influence of tool geometry, workpiece material properties, and cutting parameters.

Conclusion

The study of milling workpieces made of *Inconel 625* superalloy, produced by wire arc additive manufacturing (*WAAM*), revealed a number of key dependencies and patterns that are of practical importance for optimizing the technological process.

The microstructure of *Inconel 625* specimens formed by *WAAM* significantly affects the cutting forces. Microstructural analysis revealed a non-homogeneous distribution of hardness and grain size, caused by non-uniform heating and cooling during layer-by-layer deposition. A correlation was established between local variations in microhardness and cutting forces; increased hardness in the surface layers and specific areas of the sample led to an increase in cutting forces and more intensive tool wear compared to conventionally manufactured parts. This emphasizes the need to adapt cutting modes to the specific microstructural characteristics of workpieces produced by *WAAM* method.

Optimal cutting modes, ensuring minimization of cutting forces and tool wear, significantly depend on the specific machining parameters. For milling *Inconel 625* workpieces produced by *WAAM* technology, it is optimal to use high-strength carbide milling cutters with increased wear resistance. The application of mills with wear-resistant coatings (e.g., *TiAlN*, *AlCrN*) is possible to increase tool life. It is best to use special geometry mill cutters of a larger diameter than when machining *0.40 C-13Cr* steel. Increasing the mill cutter diameter by more than 8 mm leads to an increase in the mill cutter price proportionally to the square of the mill cutter diameter. For rough machining, consider using milling cutters with an increased helix angle to achieve a smoother entry and exit from the material and reduce vibrations. Milling is recommended to begin with low cutting speeds (e.g., at $V = 15.8$ m/min). Subsequently, the speed can be gradually increased, while controlling the cutting edge temperature and tool wear. Excessive feed rates (80 mm/min or more when feeding along the workpiece), should be avoided, especially when milling perpendicular to the deposition direction, to prevent excessive cutting forces and tool wear.

The use of conventional milling when machining *Inconel 625* alloy is categorically unacceptable, as it leads to table jerking and end mill breakage, which is especially evident at feed rates exceeding 40 mm/min. Excessive cutting speeds (above 50 m/min) when milling *Inconel 625* alloy causes the machined material to adhere to the cutter tooth due to the increased temperature in the cutting zone, which, in turn, can lead to a sharp increase in cutting forces and tool breakage.

Increasing the number of teeth while maintaining the same cutter diameter leads to chip welding to the chip helical groove and a sharp increase in temperature in the cutting zone. This is due to friction between the compressed chip material in the chip helical groove and the cutting surface, ultimately causing the cutter to failure.

The use of specialized tooling is a prerequisite for effective machining. The increased abrasiveness and heterogeneity of *Inconel 625* workpieces produced by *WAAM* require the use of high-strength carbide milling cutters with enhanced wear resistance and, potentially, a specialized geometry. The empirical relationships developed in this study, along with recommendations for tool selection and cutting parameter optimization for milling *Inconel 625* workpieces produced by *WAAM*, will improve the efficiency and productivity of machining additively manufactured parts. However, further research is needed for a deeper understanding of the influence of residual stresses and the development of methods for their control. This will enable the optimization of milling processes to achieve high levels of surface quality, productivity, and economic efficiency.



References

1. Alvarez L.F., Garcia C., Lopez V. Continuous cooling transformations in martensitic stainless steels. *ISIJ International*, 1994, vol. 34 (6), pp. 516–521. DOI: 10.2355/isijinternational.34.516.
2. Kazemipour M., Lunde J.H., Salahi S., Nasiri A. On the microstructure and corrosion behavior of wire arc additively manufactured AISI 420 stainless steel. *TMS 2020: 149th Annual Meeting & Exhibition Supplemental Proceedings*. Cham, Springer, 2020, pp. 435–448. DOI: 10.1007/978-3-030-36296-6_41.
3. Liverani E., Fortunato A. Additive manufacturing of AISI 420 stainless steel: process validation, defect analysis and mechanical characterization in different process and post-process conditions. *The International Journal of Advanced Manufacturing Technology*, 2021, vol. 117 (3–4), pp. 809–821. – DOI: 10.1007/s00170-021-07639-6.
4. Saeidi K., Zapata D.L., Lofaj F., Kvetkova L., Olsen J., Shen Z., Akhtar F. Ultra-high strength martensitic 420 stainless steel with high ductility. *Additive Manufacturing*, 2019, vol. 29, p. 100803. DOI: 10.1016/j.addma.2019.100803.
5. Krakhmalev P., Yadroitsava I., Fredriksson G., Yadroitsev I. In situ heat treatment in selective laser melted martensitic AISI 420 stainless steels. *Materials & Design*, 2015, vol. 87, pp. 380–385. DOI: 10.1016/j.matdes.2015.08.045.
6. Ge J., Lin J., Chen Y., Lei Y., Fu H. Characterization of wire arc additive manufacturing 2Cr13 part: Process stability, microstructural evolution, and tensile properties. *Journal of Alloys and Compounds*, 2018, vol. 748, pp. 911–921. DOI: 10.1016/j.jallcom.2018.03.222.
7. Manokruang S., Vignat F., Museau M., Limousin M. Process parameters effect on weld beads geometry deposited by Wire and Arc Additive Manufacturing (WAAM). *Advances on Mechanics, Design Engineering and Manufacturing III*. Proceedings of the International Joint Conference on Mechanics, Design Engineering & Advanced Manufacturing, JCM 2020, June 2–4, 2020. Cham, Springer, 2021, pp. 9–14. DOI: 10.1007/978-3-030-70566-4_3.
8. Grzesik W. Hybrid additive and subtractive manufacturing processes and systems: a review. *Journal of Machine Engineering*, 2018, vol. 18 (4), pp. 5–24. DOI: 10.5604/01.3001.0012.7629.
9. Lopes J.G., Machado C.M., Duarte V.R., Rodrigues T.A., Santos T.G., Oliveira J.P. Effect of milling parameters on HSLA steel parts produced by Wire and Arc Additive Manufacturing (WAAM). *Journal of Manufacturing Processes*, 2020, vol. 59, pp. 739–749. DOI: 10.1016/j.jmapro.2020.10.007.
10. Dang J., Zhang H., Ming W., An Q., Chen M. New observations on wear characteristics of solid $\text{Al}_2\text{O}_3/\text{Si}_3\text{N}_4$ ceramic tool in high speed milling of additive manufactured Ti6Al4V. *Ceramics International*, 2020, vol. 46 (5), pp. 5876–5886. DOI: 10.1016/j.ceramint.2019.11.039.
11. Bordin A., Bruschi S., Ghiotti A., Bariani P.F. Analysis of tool wear in cryogenic machining of additive manufactured Ti6Al4V alloy. *Wear*, 2015, vol. 328–329, pp. 89–99. DOI: 10.1016/j.wear.2015.01.030.
12. Milton S., Morandau A., Chalon F., Leroy R. Influence of finish machining on the surface integrity of Ti6Al4V produced by selective laser melting. *Procedia Cirp*, 2016, vol. 45, pp. 127–130. DOI: 10.1016/j.procir.2016.02.340.
13. Keist J.S., Palmer T.A. Development of strength-hardness relationships in additively manufactured titanium alloys. *Materials Science and Engineering: A*, 2017, vol. 693, pp. 214–224. DOI: 10.1016/j.msea.2017.03.102.
14. Tascioglu E., Kaynak Y., Poyraz Ö., Orhangül A., Ören S. The effect of finish-milling operation on surface quality and wear resistance of Inconel 625 produced by selective laser melting additive manufacturing. *Advanced Surface Enhancement (INCASE 2019)*. Singapore, Springer, 2020, pp. 263–272. DOI: 10.1007/978-981-15-0054-1_27.
15. Montevecchi F., Grossi N., Takagi H., Scippa A., Sasahara H., Campatelli G. Cutting forces analysis in additive manufactured AISI H13 alloy. *Procedia CIRP*, 2016, vol. 46, pp. 476–479. DOI: 10.1016/j.procir.2016.04.034.
16. Hojati F., Daneshi A., Soltani B., Azarhoushang B., Biermann D. Study on machinability of additively manufactured and conventional titanium alloys in micro-milling process. *Precision Engineering*, 2020, vol. 62, pp. 1–9. DOI: 10.1007/s00170-020-06391-7.
17. Gong Y., Li P. Analysis of tool wear performance and surface quality in post milling of additive manufactured 316L stainless steel. *Journal of Mechanical Science and Technology*, 2019, vol. 33 (5), pp. 2387–2395. DOI: 10.1007/s12206-019-0237-x.
18. Ni Ch., Zhu L., Yang Zh. Comparative investigation of tool wear mechanism and corresponding machined surface characterization in feed-direction ultrasonic vibration assisted milling of Ti–6Al–4V from dynamic view. *Wear*, 2019, vol. 436, p. 203006. DOI: 10.1016/j.wear.2019.203006.



19. Xiong X., Haiou Z., Guilan W. A new method of direct metal prototyping: hybrid plasma deposition and milling. *Rapid Prototyping Journal*, 2008, vol. 14 (1), pp. 53–56. DOI: 10.1108/13552540810841562.
20. Ahmetshin R., Fedorov V., Kostikov K., Martyushev N., Ovchinnikov V., Rasin A., Yakovlev A. SLS setup and its working procedure. *Key Engineering Materials*, 2016, vol. 685, pp. 477–481. DOI: 10.4028/www.scientific.net/KEM.685.477.
21. Martyushev N., Petrenko Yu. Effects of crystallization conditions on lead tin bronze properties. *Advanced Materials Research*, 2014, vol. 880, pp. 174–178. DOI: 10.4028/www.scientific.net/AMR.880.174.
22. Isametova M.E., Martyushev N.V., Karlina Y.I., Kononenko R.V., Skeebe V.Y., Absadykov B.N. Thermal pulse processing of blanks of small-sized parts made of beryllium bronze and 29 NK alloy. *Materials*, 2022, vol. 15 (19), p. 6682. DOI: 10.3390/ma15196682.
23. Martyushev N.V., Bublik D.A., Kukartsev V.V., Tynchenko V.S., Klyuev R.V., Tynchenko Y.A., Karlina Y.I. Provision of rational parameters for the turning mode of small-sized parts made of the 29 NK alloy and beryllium bronze for subsequent thermal pulse deburring. *Materials*, 2023, vol. 16 (9), p. 3490. DOI: 10.3390/ma16093490.
24. Cahoon J.R., Broughton W.H., Kutzak A.R. The determination of yield strength from hardness measurements. *Metallurgical Transactions*, 1971, vol. 2 (7), pp. 1979–1983. DOI: 10.1007/bf02913433.
25. Abootorabi Zarch M.M., Razfar M.R., Abdullah A. Influence of ultrasonic vibrations on side milling of AISI 420 stainless steel. *The International Journal of Advanced Manufacturing Technology*, 2013, vol. 66, pp. 83–89. DOI: 10.1007/s00170-012-4307-9.
26. Lou X., Andresen P.L., Rebak R.B. Oxide inclusions in laser additive manufactured stainless steel and their effects on impact toughness and stress corrosion cracking behavior. *Journal of Nuclear Materials.*, 2018, vol. 499, pp. 182–190. DOI: 10.1016/j.jnucmat.2017.11.036.
27. Chen X., Li J., Cheng X., Wang H., Huang Z. Effect of heat treatment on microstructure, mechanical and corrosion properties of austenitic stainless steel 316L using arc additive manufacturing. *Materials Science and Engineering: A*, 2018, vol. 715, pp. 307–314. DOI: 10.1016/j.msea.2017.10.002.
28. Martyushev N.V., Kozlov V.N., Qi M., Tynchenko V.S., Kononenko R.V., Konyukhov V.Y., Valuev D.V. Production of workpieces from martensitic stainless steel using electron-beam surfacing and investigation of cutting forces when milling workpieces. *Materials*, 2023, vol. 16 (13), p. 4529. DOI: 10.3390/ma16134529.
29. Shlyakhova G.V., Bochkareva A.V., Barannikova S.A., Zuev L.B., Martusevich E.V. Vozmozhnosti atomno-silovoi mikroskopii dlya issledovaniya mikrostruktury nerzhavayushchei stali pri razlichnykh vidakh termoobrabotki [Application of atomic force microscopy for stainless steel microstructure study at various kinds of heat treatment]. *Izvestiya vysshikh uchebnykh zavedenii. Chernaya Metallurgiya = Izvestiya. Ferrous Metallurgy*, 2017, vol. 60 (2), pp. 133–139. DOI: 10.17073/0368-0797-2017-2-133-139.
30. Haidorov A.D., Yunusov F.A. Vakuumnaya termicheskaya obrabotka vysokolegirovannykh korroziionostoikikh stali [Vacuum heat treatment of high alloy corrosion-resistant steels]. *Nauchno-tekhnicheskie vedomosti SPbGPU = St. Petersburg polytechnic university journal of engineering sciences and technology*, 2017, vol. 23 (1), pp. 226–235. DOI: 10.18721/JEST.230123.
31. Kondrakhin V.P., Klyuev R.V., Sorokova S.N., Efremkov E.A., Valuev D.V., Mengxu Q. Mathematical modeling and multi-criteria optimization of design parameters for the gyratory crusher. *Mathematics*, 2023, vol. 11, p. 2345. DOI: 10.3390/math11102345.

Conflicts of Interest

The authors declare no conflict of interest.

© 2025 The Authors. Published by Novosibirsk State Technical University. This is an open access article under the CC BY license (<http://creativecommons.org/licenses/by/4.0>).